

# Far-infrared spectra of lateral quantum dot molecules

**M. Helle, A. Harju, and R. M. Nieminen**

Laboratory of Physics, Helsinki University of Technology, P. O. Box 4100  
FIN-02015 HUT, Finland

**Abstract.**

We study effects of electron-electron interactions and confinement potential on the magneto-optical absorption spectrum in the far-infrared range of lateral quantum dot molecules. We calculate far-infrared (FIR) spectra for three different quantum dot molecule confinement potentials. We use accurate exact diagonalization technique for two interacting electrons and calculate dipole-transitions between two-body levels with perturbation theory. We conclude that the two-electron FIR spectra directly reflect the symmetry of the confinement potential and interactions cause only small shifts in the spectra. These predictions could be tested in experiments with nonparabolic quantum dots by changing the number of confined electrons. We also calculate FIR spectra for up to six noninteracting electrons and observe some additional features in the spectrum.

## 1. Introduction

Far-infrared (FIR) magneto-optical absorption spectroscopy is one experimental technique to study electrons confined in semiconductor quantum dots (QDs) [1, 2]. It was, however, realized at the early stage of QD research that FIR spectroscopy is unable to reveal interesting many-electron effects in parabolic-confinement QDs. This is because the electromagnetic waves couple only to the center-of-mass variables of electrons. The resulting FIR spectrum is rather simple, showing two branches,  $\omega_{\pm}$ , as a function of magnetic field [3, 4]. These branches, one with positive energy dispersion ( $\omega_{+}$ ) and one with negative energy dispersion ( $\omega_{-}$ ) as a function of magnetic field, are called the Kohn modes. The spectrum does not depend on the number of electrons nor on the interactions between them. This condition in parabolic QDs is called the generalized Kohn theorem [5]. The condition can be lifted if the confinement is not parabolic, and many experiments show more complex FIR spectra [1, 6, 7, 8]. Also calculations [9, 10, 11, 12, 13, 14, 15, 16] have shown non-trivial FIR spectra of non-parabolic QDs. It is also possible that spin-orbit interaction [17] and impurities near quantum dots [18] can have an effect on the FIR spectrum. In a nonparabolic QD, the relative internal motion of electrons could be accessible with the FIR spectroscopy, but recent studies suggest that additional features in the FIR spectra are still of collective nature [9]. The interpretation of the observed FIR spectra of a nonparabolic QD is usually far from trivial. It is clear that deviations arise from nonparabolic confinement, but the detailed cause of the deviations, thus the interpretation of spectrum, is not always straightforward. It is especially interesting to see how many-electron interactions appear in the FIR spectra of QDs.

In the calculation of FIR spectra of two-electron lateral double QD [9] and lateral four-minima quantum dot molecule (QDM) [10] it was shown that the deviations from the Kohn modes arise mainly from nonparabolic confinement and interactions have only minor effects on the spectra. Effects of relative motion of electrons on FIR spectra were studied by turning electron-electron interactions on and off. The results indicate that the FIR spectra of QDMs reveal mainly the center-of-mass collective excitations of electrons. Actually more pronounced deviations from Kohn modes are observed when interactions between the electrons are turned off. This is an interesting result, suggesting that less features are observed with more electrons in a non-parabolic QD. These studies, however, include only two electrons and the FIR spectra may depend on particle number. Also as more single-particle levels are occupied the center-of-mass excitations with slightly different energies may be observed where interactions do not, necessarily, have any significant role. Calculations where electron interactions can be turned on and off could show how the electron-electron interactions show up in FIR spectra for greater electron numbers ( $N > 2$ ).

In this article we study three different lateral quantum dot molecule (QDM) confinements. We study two-minima QDM (double dot), and square-symmetric and rectangular-symmetric four-minima QDMs. We calculate the FIR spectra for all the QDM confinements and compare them to the parabolic-confinement QD FIR spectrum. We analyze in detail the effect of electron-electron interactions on the FIR spectra. We use very accurate exact diagonalization technique for interacting electrons but limit our studies to two interacting electrons. We also calculate the FIR spectra of non-interacting electrons up to six electrons by occupying single-particle levels and calculating dipole-transition elements between the single-particle levels. These provide some insight how FIR spectra are modified with greater electron numbers, even if we

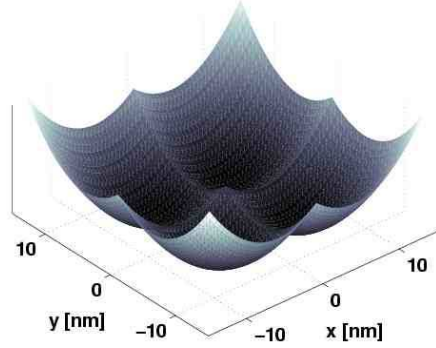


**Figure 1.** Confinement potential of square-symmetric ( $L_x = L_y = 5$  nm) four-minima quantum dot molecule.

do not include electron-electron interactions. Especially if excitations are collective also with the greater electron numbers, the FIR spectra are basically given by the transitions between single-particle levels of the quantum dot confinement in question.

## 2. Model and method

We model the interacting two-electron quantum-dot molecule with a two-dimensional Hamiltonian

$$H = \sum_{i=1}^2 \left( \frac{(-i\hbar\nabla_i - \frac{e}{c}\mathbf{A})^2}{2m^*} + V_c(\mathbf{r}_i) \right) + \frac{e^2}{\epsilon r_{12}}, \quad (1)$$

where  $V_c$  is the external confinement potential of the QDM taken to be

$$V_c(\mathbf{r}) = \frac{1}{2}m^*\omega_0^2 \min \left\{ \sum_j^M (\mathbf{r} - \mathbf{L}_j)^2 \right\}. \quad (2)$$

The coordinates are in two dimensions  $\mathbf{r} = (x, y)$ , the  $\mathbf{L}_j$ 's ( $\mathbf{L}_j = (L_x, L_y)$ ) give the positions of the minima of QDM potential, and  $M$  is the number of minima. When  $\mathbf{L}_1 = (0, 0)$  (and  $M = 1$ ) we have a single parabolic QD. With  $M = 2$  and  $\mathbf{L}_{1,2} = (\pm L_x, 0)$  we get a double-dot potential. We also study four-minima QDM ( $M = 4$ ) with minima at four possibilities of  $(\pm L_x, \pm L_y)$  (see Fig. 1). We study both square-symmetric ( $L_x = L_y$ ) and rectangular-symmetric ( $L_x \neq L_y$ ) four-minima QDMs. The confinement potential can also be written using the absolute values of  $x$  and  $y$  coordinates as

$$V_c(x, y) = \frac{1}{2}m^*\omega_0^2 \times [r^2 - 2L_x|x| - 2L_y|y| + L_x^2 + L_y^2]. \quad (3)$$

For non-zero  $L_x$  and  $L_y$ , the perturbation to the parabolic potential comes from the linear terms of  $L_x$  or  $L_y$  containing also the absolute value of the associated coordinate.

We use the GaAs material parameters  $m^*/m_e = 0.067$  and  $\epsilon = 12.4$ , and confinement strength  $\hbar\omega_0 = 3.0$  meV. This confinement corresponds to harmonic oscillator strength of  $l_0 = \sqrt{\hbar/\omega_0 m^*} \approx 20$  nm. We concentrate on closely coupled

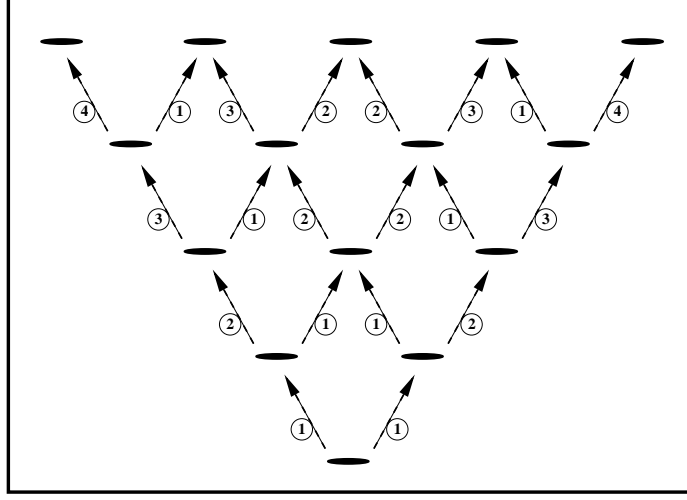


**Figure 2.** Relative transition probabilities between Fock-Darwin energy levels  $P = \langle \phi_{n',l\pm 1} | e^{\pm i\phi} \mathbf{r} | \phi_{n,l} \rangle$ .

QDMs where  $L_{x,y} \leq l_0$ . The magnetic field (in  $z$  direction) is included in the symmetric gauge by vector potential  $\mathbf{A}$ . The Hamiltonian of Eq. (1) is spin-free, and the Zeeman energy can be included in the total energy afterwards ( $E_Z = g^* \mu_B B S_Z$  with  $g^* = -0.44$  for GaAs). We disregard the threefold splitting of each triplet state ( $S_Z = 0, \pm 1$ ) and consider only the lowest energy one ( $S_Z = 1$ ).

We exclude the explicit spin-part of the wave function and expand the many-body wave function in symmetric functions for the spin-singlet state ( $S = 0$ ) and anti-symmetric functions for the spin-triplet state ( $S = 1$ ).

$$\begin{aligned} \Psi_S(\mathbf{r}_1, \mathbf{r}_2) = & \sum_{i \leq j} \alpha_{i,j} \{ \phi_i(\mathbf{r}_1) \phi_j(\mathbf{r}_2) \\ & + (-1)^S \phi_i(\mathbf{r}_2) \phi_j(\mathbf{r}_1) \}, \end{aligned} \quad (4)$$

where  $\alpha_{i,j}$ 's are complex coefficients. The one-body basis functions  $\phi_i(\mathbf{r})$  are 2D Gaussians.

$$\phi_{n_x, n_y}(\mathbf{r}) = x^{n_x} y^{n_y} e^{-r^2/2}, \quad (5)$$

where  $n_x$  and  $n_y$  are positive integers. The complex coefficient vector  $\alpha_{i,j}$  of  $\Psi_l$  and the corresponding energy  $E_l$  are found from the generalized eigenvalue problem where the overlap ( $S$ ) and Hamiltonian ( $H$ ) matrix elements are calculated analytically ( $H\alpha_l = E_l S\alpha_l$ ). The matrix is diagonalized numerically.

The FIR spectra are calculated as transition probabilities from ground state ( $E_0$ ) to excited states ( $E_l$ ) using the Fermi golden rule within the electric-dipole approximation:

$$\mathcal{A}_{l\pm} \propto \left| \left\langle \Psi_l \left| e^{\pm i\phi} \sum_{i=1}^2 \mathbf{r}_i \right| \Psi_0 \right\rangle \right|^2 \delta(E_l - E_0 - \hbar\omega). \quad (6)$$

We assume circular polarization of the electromagnetic field:  $e^{\pm i\phi} \sum_i \mathbf{r}_i = \sum_i (x_i \pm iy_i) = z_{\pm}$ , where plus indicates right-handed polarization and minus left-handed

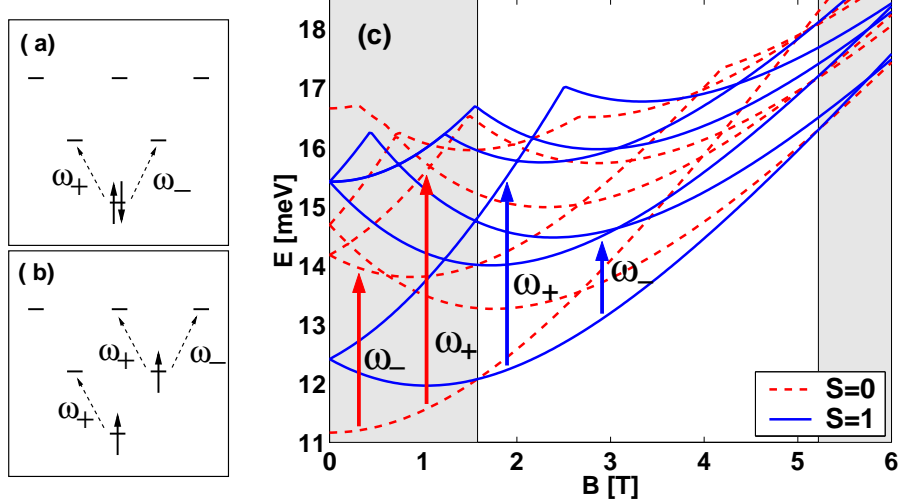


**Figure 3.** Transitions for spin singlet (a) and spin triplet (b). (c) Two-particle energy levels of a parabolic quantum dot. Red lines show singlet energy levels and blue lines triplet energy levels. Gray background shows singlet ground state regions and white triplet ground state regions. Dipole transitions from one spin type to another are forbidden.

polarization. The results are presented for non-polarized light as an average of the two circular polarizations.

### 3. Far-infrared spectra of two-electron quantum-dot molecules

The dipole-allowed magneto-optical excitation spectrum of an isolated harmonic-confined QD consist of two branches  $\omega_+$  and  $\omega_-$ , whose energy dispersion is well understood and does not depend on the number of electrons in the quantum dot:

$$\Delta E_{\pm} = \hbar\omega_{\pm} = \hbar\sqrt{\omega_0^2 + (\omega_c/2)^2} \pm \hbar\omega_c/2. \quad (7)$$

$\omega_0$  describes the external confinement,  $\omega_c = eB/m^*$  is the cyclotron frequency, and  $m^*$  is the effective mass of electron. Fock-Darwin energy levels as a function of magnetic field are given by  $E_{nl} = (2n + |l| + 1)\hbar\omega - \frac{1}{2}l\hbar\omega_c$ , where  $n = 0, 1, 2, \dots$  and  $l = 0, \pm 1, \dots$  are principal and azimuthal quantum numbers, respectively, and  $\omega = \sqrt{\omega_0^2 + (\omega_c/2)^2}$ . In the dipole-allowed transitions between Fock-Darwin states angular momentum must change by unity,  $\Delta l = \pm 1$ . Fig. 2 shows relative transition probabilities between Fock-Darwin energy levels  $P = \langle \phi_{n', l \pm 1} | e^{\pm i\phi} \mathbf{r} | \phi_{n, l} \rangle$ .

For a two-electron QD the ground state can be either spin singlet ( $S = 0$ ) or spin triplet ( $S = 1$ ) depending on the magnetic field strength. Even if many-body energy levels have more complicated magnetic field dispersion than the single-particle levels, the dipole-transitions in the many-body case always equal to transitions between the single-particle levels in a *parabolic* confinement. A schematic picture of transitions at zero magnetic field is shown in Fig. 3 (a) and (b) for spin-singlet and spin-triplet states, respectively. Fig. 3 (c) shows a few lowest two-body energy levels as a function of magnetic field for the singlet and triplet states of a parabolic QD. The gray background

marks the magnetic field region of the spin-singlet ground state and white the spin-triplet ground state. Dipole transitions from one spin type to another are forbidden.

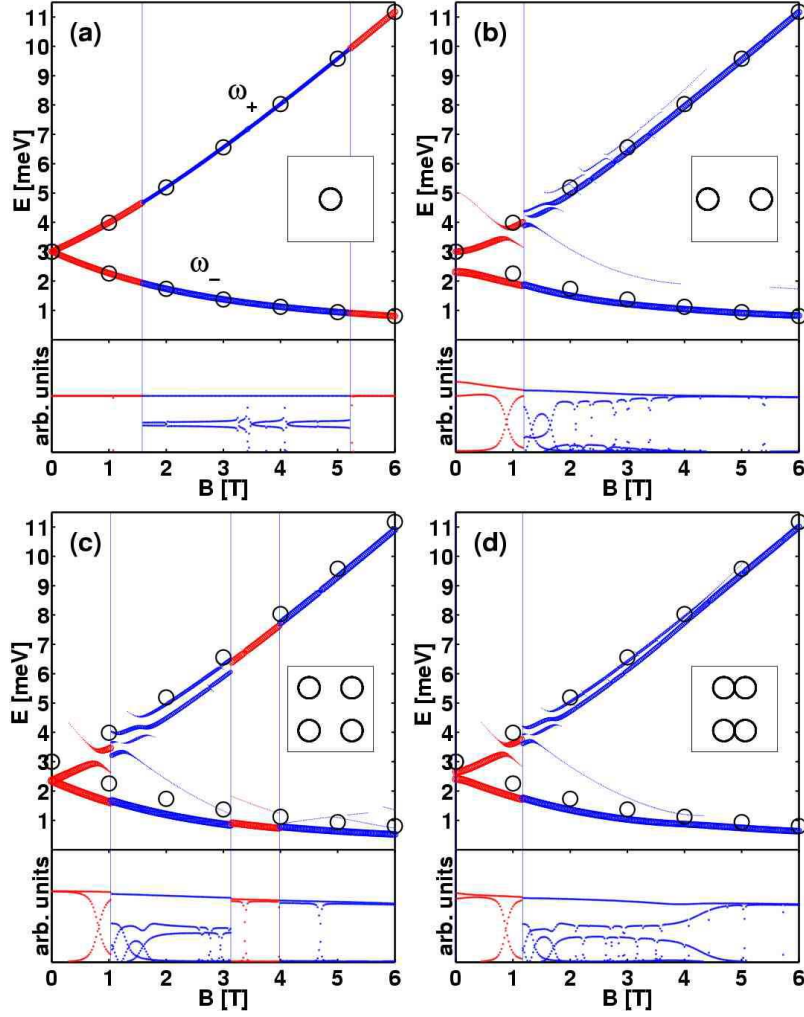
### 3.1. Interacting two-electron spectra

Fig. 4 shows the calculated far-infrared (FIR) absorption spectra for two interacting electrons. Fig. 4 (a) shows the FIR spectrum for parabolic QD, (b) for two-minima QDM (double dot), (c) for square symmetric four-minima QDM and (d) for rectangular-symmetric four-minima QDM. The energy of absorbed light is given in meV as a function of magnetic field. The width of the line is proportional to the transition probability, which is also plotted below each spectrum (in arbitrary units) for each of the branches in the spectrum. There are, of course, many more possible transitions with nearly zero or small probability. Only the lines with transitions probability exceeding 1% of the maximum transition probability are included in Fig. 4. Large open circles in the spectra represent the two Kohn modes,  $\omega_+$  and  $\omega_-$ , plotted with 1T spacings. In QDMs there are ground state transitions from spin-singlet ( $S = 0$ ) to spin-triplet ( $S = 1$ ) ground states, and the other way round, as a function of magnetic field [19, 20]. Vertical lines indicate the singlet-triplet (or triplet-singlet) transition points and the singlet ground state regions of spectrum are marked with red color and the blue lines denote triplet regions. Dipole transitions from one spin type to another are forbidden.

Fig. 4 (a) shows the calculated FIR spectra for a single parabolic QD. The dipole transition probabilities are calculated from the two-body ground state level to higher two-body energy levels as shown in Fig. 3 (c). The spectrum of Fig. 4 (a) shows two Kohn modes  $\omega_+$  and  $\omega_-$ . These coincide perfectly with the open circles presenting Kohn modes, as they should, since in a parabolic QD the FIR spectra does not depend on the number of electrons in the QD nor on the interactions between them [5]. The magnitude of the absorbed light can only change when the number of electrons in the QD is changed [1, 4]. However, in the two-electron QD of Fig. 4 (a) the width of the upper branch is halved after the first singlet triplet transition. The transition line is split into two degenerate transitions with almost equal transition probabilities, which, if summed up, would equal to the transition probability of  $\omega_-$ . In the calculations we can identify two degenerate levels to which electrons can be excited (see Fig. 3 (b)), but in experiments the observed quantity is the overall absorption of the energy in question. Therefore one can observe Kohn modes with constant transition probabilities as a function of magnetic field.

Fig. 4 (b), (c), and (d) show FIR spectra for quantum-dot molecules. Now as the symmetry of the confinement is lower, the center of mass and relative motion do not decouple. There are clear deviations from the Kohn modes. In all of the QDM potentials we can see some general features. The main branches of the spectra always lie below the Kohn modes (below open circles). There are clear anticrossings and the upper branch is split to two in some parts of the triplet spectra.

In the double dot spectra of Fig. 4 (b), the excitations at zero magnetic field are identified to a lower energy one along the long axis (the line connecting two dots,  $x$  axis) and a higher energy one along the short axis ( $y$  axis). This can be also verified by calculating the absorption of linearly polarized light [9]. At  $B = 0$  the excitation of  $\omega_+$  is unaffected by the interactions between electrons and coincides with the confinement ( $\hbar\omega_0 = 3$  meV), because in the double dot the potential is still parabolic along the  $y$  axis. However, with non-zero  $B$  this is no longer true since a magnetic field mixes



**Figure 4.** Calculated far-infrared spectra of single parabolic quantum dot in (a), double dot with  $L_x = 15$  nm in (b), square-symmetric four-minima quantum-dot molecule with  $L_x = L_y = 10$  nm in (c), and rectangular-symmetric four-minima quantum-dot molecule with  $L_x = 5, L_y = 10$  nm in (d). The energy of absorbed light is given in meV as a function of magnetic field. The width of the line is proportional to the transition probability, which is also plotted below each spectrum (in arbitrary units) for each of the branches in the spectrum. Transitions with small probability are excluded from the spectra. Only the lines with transitions probability exceeding one percent of the maximum transition probability are included in the spectra. Large open circles in the spectra represent two Kohn modes plotted with one tesla spacings. Vertical lines indicate the singlet-triplet (or triplet-singlet) transition points.

the two linear polarizations. At high magnetic field the spectrum approaches Kohn modes and no anticrossings are observed. In the high field region the electrons are effectively more localized into individual dots [20]. Then the non-parabolic nature of the confinement potential has a less important role, since the electron density is more localized close to the parabolic minima.

After the singlet-triplet transition there appears an additional level,  $\omega_{+2}$ , above  $\omega_+$  with a lower transition probability. A simple explanation for two positive dispersion levels would be in the picture of Fig. 3 (b) where the two transitions of  $\omega_+$  mode could have slightly different energy difference in a non-parabolic confinement. However, the interpretation is not so straightforward, since the dipole transitions are calculated between two-body levels and not occupied single-particle levels, as we will see when we analyze interactions in the next subsection. Another deviation from the Kohn modes of a parabolic QD are seen as small discontinuities in the energy of the spectral lines when the singlet changes to triplet. However, this discontinuity is very small and may not be resolved in experiments. See Ref. [9] for more details on double dot FIR spectra.

In the square-symmetric four-minima QDM (Fig. 4 (c)) the potential is identical in  $x$  and  $y$  directions resulting in only one excitation at  $B = 0$  as the long and short axes are equal. This excitation is clearly lower than the  $\hbar\omega_0 = 3$  meV confinement energy of a single minimum. The upper branch is split to two levels in the first triplet region at magnetic field values between 1 and 3 T, but in the second triplet region  $B > 4$  T there is only one upper branch. In square-symmetric four-minima QDM the two levels of the split-off upper branch have almost equal transition probabilities. Discontinuities in the spectra appear in the singlet-triplet (or triplet-singlet) transition points. A brief representation of the FIR spectra of square-symmetric four-minima QDM can also be found in Ref. [10].

The spectrum of rectangular-symmetric four-minima QDM, in Fig. 4 (d), has similar features as the double dot spectra. There is a gap between the two branches at  $B = 0$ . The lower branch at  $B = 0$  in Fig. 4 (d) corresponds to excitation along  $y$  axis and the upper branch along  $x$  axis. The upper mode does not start at 3 meV, as in the double dot, since the potential is not parabolic in  $x$  direction. After the singlet-triplet transition an additional mode,  $\omega_{+2}$ , appears above  $\omega_+$ . The transition probability of  $\omega_{+2}$  is higher compared to the  $\omega_{+2}$  of double dot, but the transition probability is not as high as in the square-symmetric four-minima QDM. The modes of Fig. 4 (d) at high magnetic field do not become so close to Kohn modes as in the double dot. The reason is that electrons localize into two decoupled double dots rather than into single QDs as in the double dot spectrum of Fig. 4 (b).

All QDM confinements show anticrossings in  $\omega_+$ . The clearest anticrossings are seen at low magnetic field strengths. At higher  $B$  there are still anticrossings but the energy gap is so small that they are not visible in the spectra. The transition probabilities in the lower panels, however, reveal anticrossings as the transition probability of one mode decreases and the other one increases as a function of magnetic field. The biggest anticrossing gap in energy is seen with square-symmetric four-minima QDM. This is interesting, since in our previous studies the square-symmetric four-minima QDM resembled the most a parabolic QD whereas double dot and rectangular four-minima QDM showed greater deviations in the ground state properties and in the low-lying eigenstates [20]. Obviously this is not true with the excitation spectrum and with the higher eigenstates.



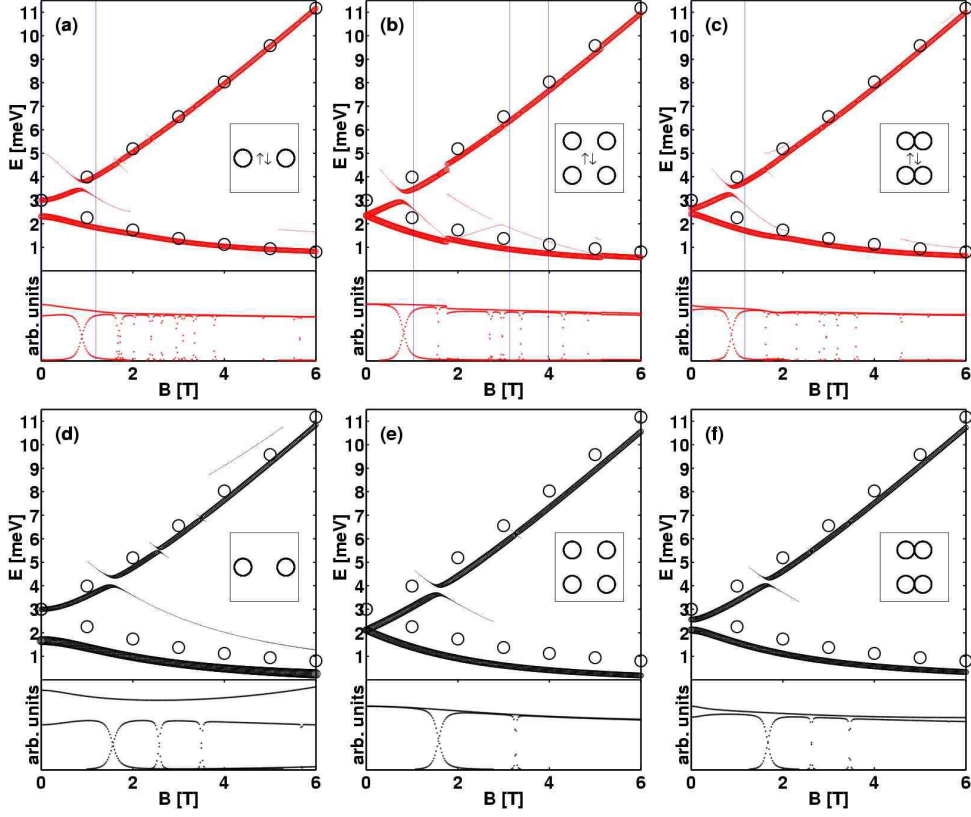


**Figure 5.** Far-infrared spectra of two interacting electrons in the singlet symmetry in (a)-(c) for double dot, square-symmetric four-minima quantum-dot molecule, and rectangular-symmetric four-minima quantum-dot molecule, respectively. (d)-(f) show corresponding non-interacting far-infrared spectra.

### 3.2. Analysis of interactions in two-electron FIR spectra

We conclude that different types of deviations appear in the spectrum when the confinement potential is not perfectly parabolic. In order to analyze these deviations in more detail, we plot the full spectra up to 6 T magnetic field for both singlet and triplet states with two interacting electrons and also for two noninteracting electrons for the comparison. We are interested to see which features in the spectra are due to electron-electron interactions and which result from the lower symmetry of the confinement potential. It is also interesting to see if some features in the spectra can be used to identify the confinement potential. This would be useful for experiments where the profile of the underlying confinement potential is not clear.

We will first analyze the two-electron singlet spectra shown in Fig. 5 (a)-(c) for interacting electrons and in (d)-(f) for noninteracting electrons. The two-electron triplet spectra are shown in Fig. 6 (a)-(c) and the corresponding noninteracting spectra in (d)-(f). In a real two-electron QDM system, singlet-triplet transitions must be taken into account and therefore experimentally observable spectra for two interacting electrons are shown in Fig. 4. As the non-interacting singlet spectra, in Fig. 5 (d)-(f), are the same as the single-particle spectra, these would correspond to experimental

FIR spectra with one electron in the QDM. The non-interacting triplet, on the other hand, corresponds the FIR spectra of two occupied single-particle levels.

The double dot singlet spectrum in Fig. 5 (a) looks qualitatively very similar to the noninteracting spectrum in Fig. 5 (d). The first difference is that the Kohn modes lie at the lower energy in the non-interacting spectra compared to the interacting spectra. The only exception is in the upper mode at  $B = 0$  where both have excitation energy of  $\hbar\omega_0 = 3$  meV. In zero magnetic field this corresponds to linearly polarized excitation along  $y$  axis where the potential is parabolic and therefore excitations are not affected by the electron-electron interactions [9]. Another difference is the zero-field gap between Kohn modes which is clearly greater in the non-interacting case. Higher energy excitations in the interacting case can be explained with the Coulomb repulsion between the electrons. Coulomb repulsion effectively steepens the confinement resulting in higher excitation energies. The anticrossing points are also affected by interactions whereas the gap remains almost the same. The anticrossings can be seen at lower magnetic field values in the interacting spectrum. Qualitatively the two spectra look very similar and we conclude that the deviations observed in the spectrum result from the low symmetry confinement and interactions only shift the excitation energies and change the anticrossing points.

Generally the same conclusions drawn for the double dot hold for the square-symmetric four-minima QDM singlet spectra in Fig. 5 (b) and (e). Now in the square-symmetric four-minima QDM the zero field excitation is degenerate as the two perpendicular directions ( $x$  and  $y$ ) have identical confinement profiles. Interactions shift the zero field excitation to higher energy due to Coulomb repulsion. The first anticrossing is again seen at lower  $B$  in the interacting spectrum. However, this time the anticrossing gap is somewhat greater in the interacting case. As a new feature, compared to the double dot, there are now discontinuities in the interacting spectrum. The discontinuities in (b) are at the transition points when two singlet states with a different symmetry cross. At  $B \approx 1.8$  T the lowest-energy singlet state changes from no-vortex state to two-vortex state and the discontinuity at  $B \approx 5.2$  T is at the crossing point of two-vortex and four-vortex states (see Ref. [20] for more details on vortex states). However, the discontinuities are seen at the magnetic field values where the true ground state is triplet and therefore the discontinuities in Fig. 5 (b) would not be observed in FIR experiments.

In the rectangular-symmetric four-minima QDM (Fig. 5 (c) and (f)) the confinement profile is non-identical and non-parabolic in both perpendicular directions. Therefore both zero-field excitations are lower than 3 meV and there is also a gap between the two modes. Again excitation energies as a function of magnetic field are higher in the interacting spectrum and anticrossings are seen at the lower magnetic field values compared to the noninteracting spectrum. Interesting point, when comparing interacting and noninteracting spectra, is that the zero-field excitation energy of the lower mode shifts to 0.30 meV higher and the higher mode shifts only 0.09 meV higher when the interactions are turned on. It means that the Coulomb repulsion is over three times more significant in the excitation along the long axis ( $y$  axis) than it is along the short axis ( $x$  axis). Electrons are localized into two distant double dots. Coulomb repulsion is more important between the two double dots as it is inside one double dot, *i.e.*, along long and short axes.

Next, we do similar comparisons for the triplet spectra of QDMs. The interacting spectra are shown in Fig. 6 (a)-(c) and non-interacting in Fig. 6 (d)-(f). We will first compare double dot interacting triplet spectra of Fig. 6 (a) to the noninteracting

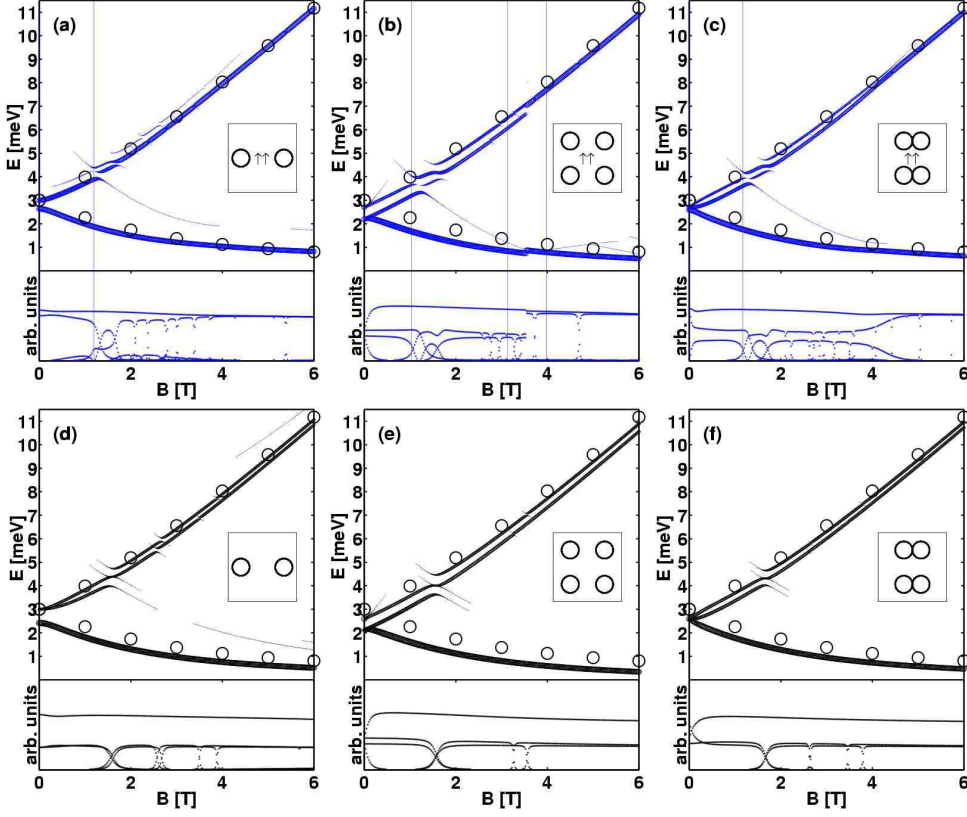


**Figure 6.** Far-infrared spectra of two interacting electrons in the triplet symmetry in (a)-(c) for double dot, square-symmetric four-minima quantum-dot molecule, and rectangular-symmetric four-minima quantum-dot molecule, respectively. (d)-(f) show the corresponding non-interacting far-infrared spectra.

spectra of Fig. 6 (d). In general, the same analysis applies to triplet spectra as for the singlet spectra of double dot. However, in the triplet state there is an additional mode,  $\omega_{+2}$ , above the main branch,  $\omega_{+}$ , in Fig. 6(a). The additional mode has clearly weaker transition probability than the  $\omega_{+}$  mode. In the noninteracting case the upper mode is split to two modes which both have equal transition probabilities. In the interacting spectrum the upper mode has lower transition probability and soon after 4 T it completely vanishes from the spectrum.

In the square-symmetric four-minima QDM also the interacting triplet spectrum, as well as the non-interacting spectrum, has two upper modes with almost equal transition probabilities (Fig. 6 (b)). In four-minima QDM the split-off branch suddenly changes to one mode at  $B \approx 3.5$  T. There the triplet ground state changes from the one-vortex to three-vortex solution (see Ref. [20] for more details on vortex states). Now the two triplet states actually cross and there occurs a discontinuity in the FIR spectrum. Yet as the singlet is the true ground state of the square-symmetric four-minima QDM between  $B \approx 3$  and 4 T, the discontinuity of Fig. 6 (b) cannot be seen in experiments. In triplet spectra there are much smaller differences between the excitation energies of interacting and noninteracting electrons compared to the singlet

spectra. In the singlet state electrons of opposite spins can occupy the same single-particle levels in the many-body configurations and therefore Coulomb repulsion is more significant for the singlet state. In other words, the Pauli exclusion principle keeps the same-spin electrons further apart and therefore Coulomb repulsion has a lesser effect on the triplet state compared to the singlet state.

In the rectangular-symmetric four-minima QDM, the zero-field gap is really small and not visible in the interacting spectra of Fig. 6 (c) and neither in the non-interacting triplet spectra of Fig. 6 (f). The transition probabilities of the two main branches ( $\omega_+$  and  $\omega_-$ ), in the interacting spectrum, are almost equal at zero field, but soon after the magnetic field strength increases the transition probability of  $\omega_+$  decreases at the same time as the transition probability of  $\omega_{+2}$  increases. After  $B = 4$  T the  $\omega_{+2}$  starts to weaken again as the symmetry of the triplet ground state is changing. The  $\omega_{+2}$  dies out continuously. The two upper modes of the non-interacting spectrum have almost equal transition probabilities. The interacting modes are higher in energy, also at  $B = 0$ , and anticrossings shift to lower  $B$  in the interacting spectrum. Anticrossing gaps are not noticeably affected by the interactions.

#### 4. FIR spectra of noninteracting electrons

A general conclusion drawn above is that the noninteracting spectra show more deviations from the Kohn modes than the interacting spectra. All the same features are present in noninteracting and interacting spectra. In addition, the non-interacting spectra show in all cases similar structure as the interacting spectra. Interactions only shift some of the features seen in the spectra. Therefore we calculate FIR spectra of non-interacting electrons up to  $N = 6$  electrons in the QDMs to see if more electrons, even if non-interacting, produce changes in the FIR spectra.

Before presenting the FIR spectra we plot single-particle energy levels of all three QDM confinements in Fig. 7. The solid lines show QDM energy levels and the dotted lines Fock-Darwin energy levels of a parabolic QD. In QDMs the energy levels shift to lower energies compared to parabolic QD. Also many anticrossings and zero-field splittings of energy levels are visible in QDMs.

We obtain noninteracting FIR spectra of QDMs by occupying lowest single-particle energy levels with  $N$  non-interacting electrons and calculating dipole transitions to higher unoccupied levels. The noninteracting FIR spectra are shown in Figs. 8, 9 and 10 for a double dot, square-symmetric four-minima QDM and rectangular-symmetric four-minima QDM, respectively. (a) to (d) correspond to FIR spectra of  $N = 1$  to  $N = 6$  electrons confined in a QDM.  $N = 1$  and  $N = 2$  are also shown in Figs. 5 and 6. The transition probabilities are multiplied when more electrons are added in the QDM. We divide each transition probability with  $N$  in order to ease comparisons.

We will first analyze the single-particle spectra of a double dot. Fig. 8 (c) for  $N = 3$  shows an additional mode below  $\omega_-$  in the low-field region with the excitation energy below  $E = 2$  meV. Also another mode is visible with a small transition probability which has zero excitation energy at  $B \approx 0.9$  T. If we study the single-particle energy levels of Fig. 7 (a), one can see that with the three lowest levels occupied, the uppermost levels cross at  $B \approx 0.9$  T. When these levels cross, the weak mode has excitation energy of  $\Delta E = 0$  and the transition probability with the  $E \leq 2$  meV mode vanishes. Another feature that is observed with  $N = 3$ , but absent in two-particle spectra, is an anticrossing in  $\omega_-$ . This anticrossing is opposite to the

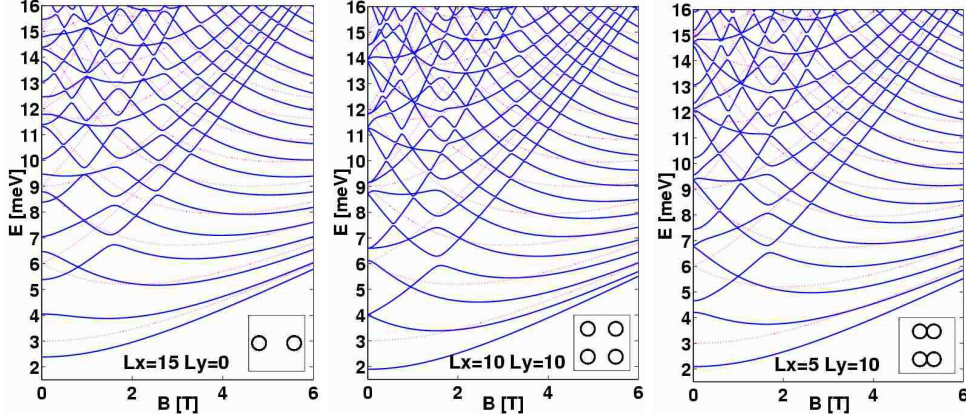


**Figure 7.** Single-particle energy levels of double dot ( $L_x = 15, L_y = 0$  nm), four-minima square-symmetric quantum-dot molecule ( $L_x = L_y = 10$  nm) and four-minima rectangular symmetric quantum-dot molecule ( $L_x = 5, L_y = 10$  nm). Dotted lines show single-particle (Fock-Darwin) energy levels of parabolic ( $\hbar\omega_0 = 3$  meV) quantum dot.

anticrossings in  $\omega_+$  where the low-field mode curves upwards and the high-field mode curves from down to up while increasing its strength.  $\omega_+$  with three electrons looks quite similar as  $\omega_+$  in  $N = 2$  spectrum.

In  $N = 4$  spectrum of Fig. 8 (d) there is one level below  $\omega_-$  at low  $B$  but the clear anticrossing, present in  $N = 3$ , is missing from the spectrum. After  $B \approx 1.7$  T there is just one lower mode. The  $N = 5$  and 6 spectra are rather featureless as clear anticrossings and additional modes are missing. There are many different levels but as they are lying close in energy, the overall spectrum resembles just two Kohn modes without clear additional features. In general, anticrossings are smaller and fewer clearly discernible additional modes are visible with  $N = 5$  and 6. Actually, there is some structure of  $\omega_-$  of  $N = 5$  and  $N = 6$  but as energies lie so close, the structure would be very difficult to observe experimentally. However, if the perturbation from parabolic potential is stronger these levels may have larger energy separation as in the experiments of Hochgräfe *et al* [7]. Another noticeable feature in the noninteracting FIR spectra of double dot is the zero field gap between the two main modes. For  $N = 1$  it clearly has the greatest value whereas for other electron numbers it does not vary much.

Fig. 9 shows non-interacting FIR spectra of square-symmetric four-minima QDM. In  $N = 3$  spectrum of Fig. 9(c) there is one additional mode below  $\omega_-$  and one anticrossing in  $\omega_-$ . The additional mode below  $\omega_-$  is much closer to  $\omega_-$  in energy as it is in the double dot spectrum. Also  $\omega_-$  has lower transition probability than the additional mode in four-minima QDM.  $N = 4, 5$  and  $N = 6$  spectra of four-minima QDM show multiple modes of  $\omega_+$  and some structure in  $\omega_-$ , but these are very close in energy and may not be resolved in experiments. However, there is a discernible split-off mode below  $\omega_+$  mode with a lower transition probability. It is difficult to say how anticrossing gaps of  $\omega_+$  at  $B \approx 1.7$  T are changing with increasing  $N$  because of multiple modes. One interesting thing is that zero-field excitation of the degenerate main branches is higher,  $E \approx 2.6$  meV, with  $N = 3 - 6$  than it is with  $N = 1$  and 2, where  $E \approx 2.1$  meV.

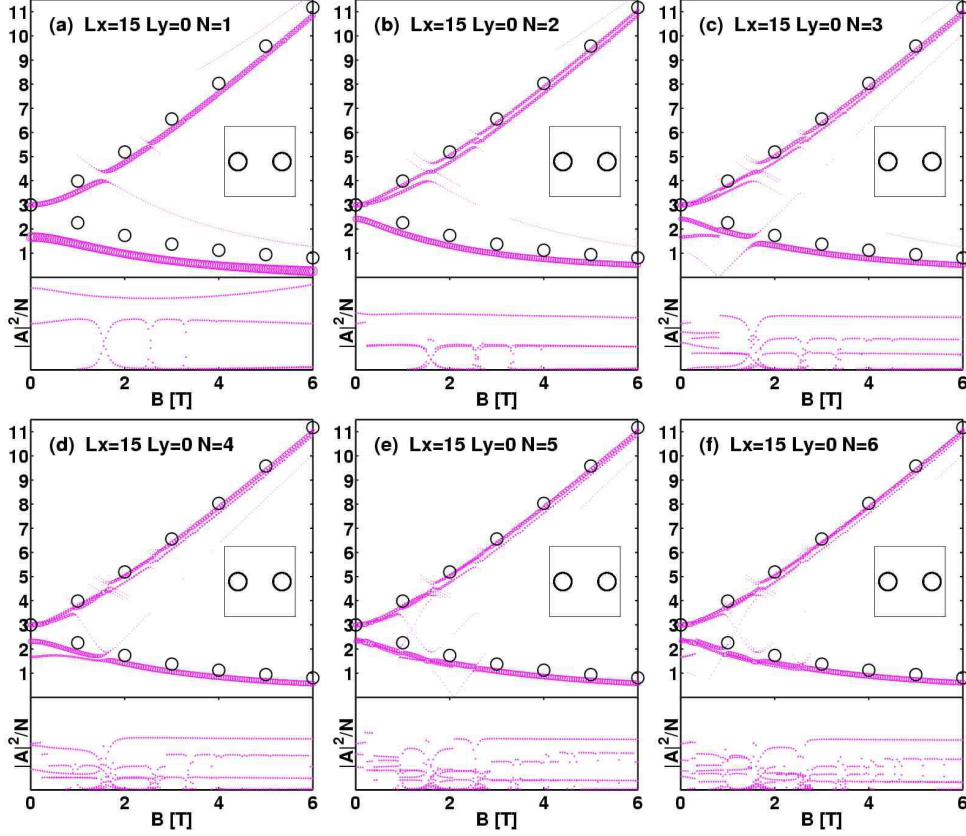


**Figure 8.** Far-infrared spectra for  $N = 1 - 6$  non-interacting electrons in double dot ( $L_x = 15, L_y = 0$  nm).

Noninteracting FIR spectra of rectangular-symmetric four-minima QDM in Fig. 10 does not deviate significantly from the FIR spectra of two other QDM confinements. Additional mode below  $\omega_-$  is very weak but visible and exist only at very low magnetic field strengths in rectangular-symmetric four-minima QDM for  $N = 3, 4$  and  $N = 6$  in Fig. 10. Clear anticrossing in  $\omega_-$  occurs only with  $N = 3$ . The zero-field gap between  $\omega_+$  and  $\omega_-$  becomes very small with more than one electron in the QDM. After the first anticrossing, at  $B \approx 2$  T, the  $\omega_+$  is split to two modes with  $N \geq 1$ , where the lower mode has lower transition probability.

## 5. Summary and conclusions

In the calculated far-infrared (FIR) spectra we are able to compare three different quantum-dot molecule (QDM) confinement potentials and study the effects of interactions on the two-electron FIR spectra. We have also calculated FIR spectra for a few noninteracting electrons. The three studied lateral QDM confinements are a two-minima QDM (double dot), and square-symmetric and rectangular-symmetric four-minima QDMs.

We observe anticrossings in the upper  $\omega_+$  mode for both interacting and



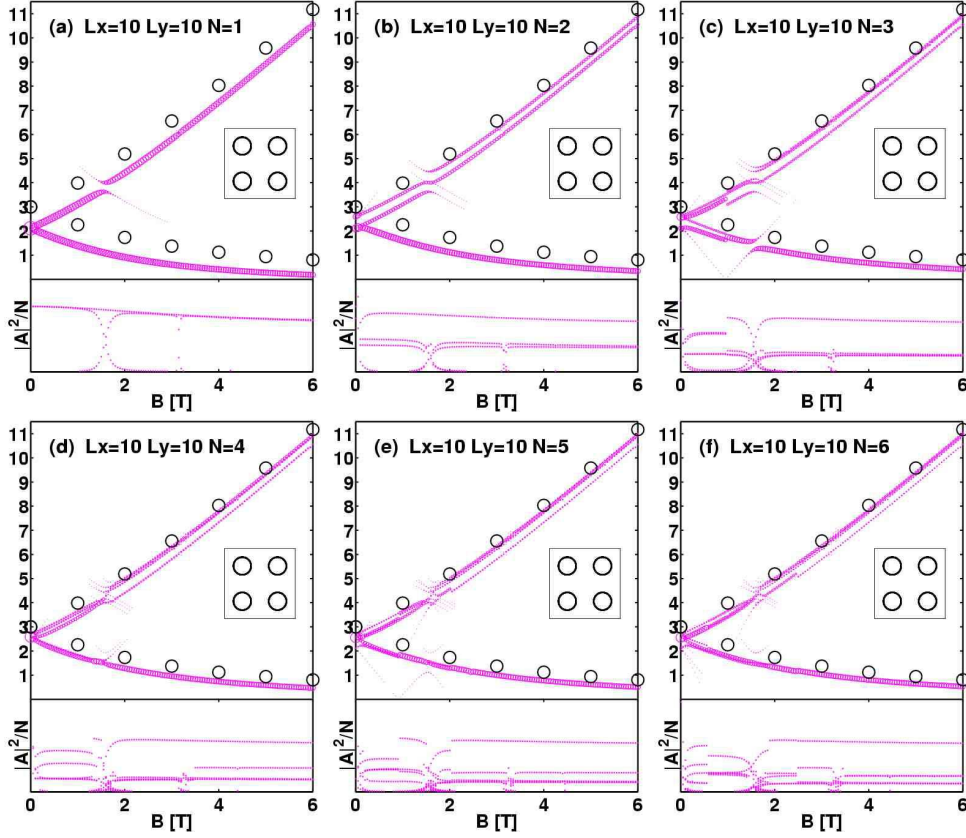


**Figure 9.** Far-infrared spectra for  $N = 1 - 6$  non-interacting electrons in square-symmetric four-minima quantum-dot molecule ( $L_x = L_y = 10$  nm).

noninteracting spectra. The anticrossing gaps are not significantly altered by the interactions, but the anticrossing positions are shifted to lower magnetic field values with the interacting electrons. When we increase the particle number in the noninteracting FIR spectra, the anticrossings in  $\omega_+$  modes become less clear as the main mode is split to multiple modes at the anticrossing point. With three noninteracting electrons ( $N = 3$ ) we see a clear anticrossing also in the lower  $\omega_-$  mode in all three QDM confinement potentials.

The  $\omega_+$  mode is split to two for  $N \geq 2$  noninteracting electrons and also in the interacting spectra when the spin-triplet is the ground state. With two interacting electrons this additional mode vanishes from the spectrum at greater magnetic field values, approximately at  $B \geq 4$  for all QDM confinements. The upper split-off mode has a lower transition probability in the interacting case in double dot and rectangular four-minima QDM confinements. In the noninteracting case, even if we add electrons up to six electrons in a QDM, the  $\omega_+$  consists of only two energy-split excitations, where one of the modes, typically the lower one, can have smaller transition probability in all three QDM confinements.

The third point that we have analyzed in the FIR spectra is the splitting between the main modes,  $\omega_{\pm}$ , at  $B = 0$ . The splitting is seen for two rectangular confinements,

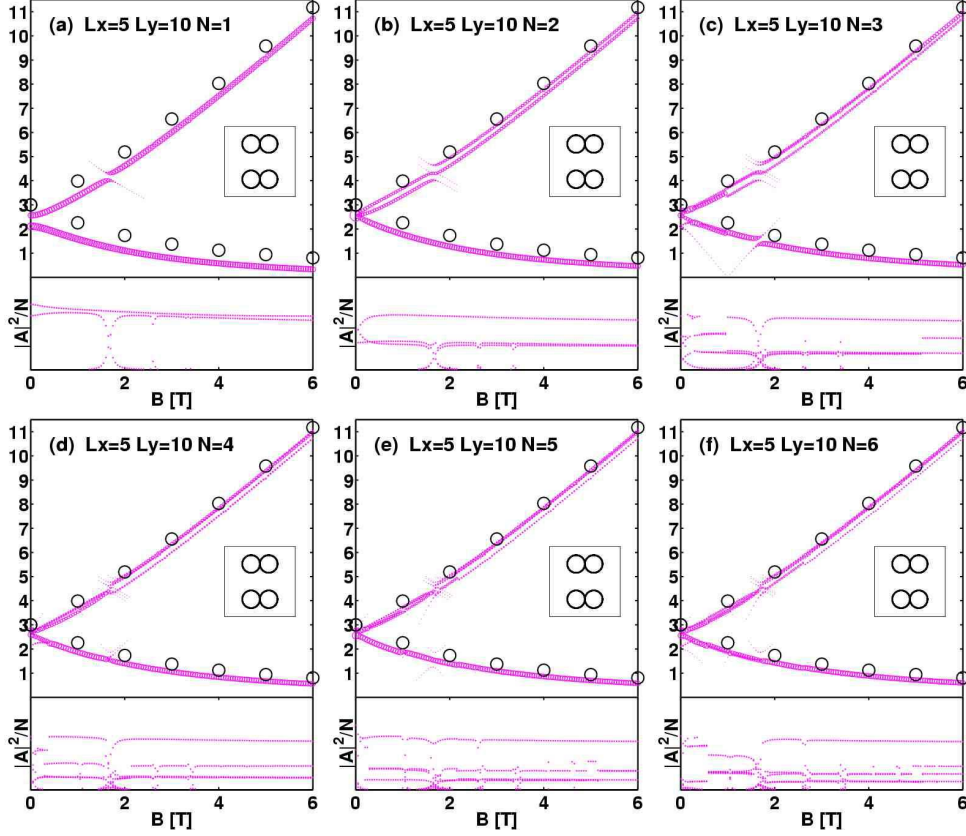


**Figure 10.** Far-infrared spectra for  $N = 1 - 6$  non-interacting electrons in rectangular four-minima QDM ( $L_x = 5, L_y = 10$  nm).

double dot and rectangular-symmetric four-minima QDM, where the excitations along short and long axes are not equal. In the two rectangular confinements, the greatest gap is seen for single electron. For all  $N \geq 2$  the gap is clearly smaller compared to  $N = 1$  but does not change significantly between  $N = 2 - 6$  noninteracting electrons in the QDM. The zero-field splitting usually diminishes as electron-electron interactions effectively steepen the potential which leads to increase in excitation energies. Interactions have stronger effect on the lower mode, which corresponds to excitation along the long axis of the confinement, therefore decreasing the gap.

Generally, QDM confinements have lower excitation energies compared to a parabolic quantum dot with the same confinement energy  $\hbar\omega_0$ . When interactions are turned on, the Coulomb repulsion effectively steepen the potential leading to a small increase in the excitation energies.

The same features are in general present in interacting and noninteracting spectra, but small shifts may occur with interacting electrons compared to the noninteracting FIR spectra. Therefore, based on calculations with two interacting electrons, we conclude that deviations from the Kohn modes are due to nonparabolic confinement potential. Interactions only shift some features in the observed spectra but otherwise excitations are of collective nature. However, this study is only for two interacting



electrons and maybe more features can be seen with more interacting electrons in a nonparabolic quantum dot confinement. Also it is possible, but unlikely, that different nonparabolic confinement potentials could show more interaction effects in FIR spectra.

We have studied how the FIR spectra change when interactions are turned on and off. These predictions could be checked in experiments when the number of electrons is increased in the dots, even if the limit of single or two electrons could not be achieved. These predictions are that *i*) anticrossings are shifted to lower magnetic field values, *ii*) excitation energies increase and *iii*) zero field gaps decrease as the Coulomb interaction increases in the quantum dot (more electrons inside dots). It is also possible that the confinement potential may change as the number of electrons changes in the dot [21]. In a rectangular symmetry also polarized light can be used to analyze excitations. These features are seen, in general terms, in elliptic quantum dots studied by Hochgräfe *et al* [7]. However, they observe a bit more complicated FIR spectra with multiple negative and positive dispersion Kohn modes.

This work has been supported by the Academy of Finland through its Centers of Excellence Program (2000-2005).

## References

- [1] Heitmann D and Kotthaus J P 1993 *Physics Today* **June** 56
- [2] Jacak L, Hawrylak P and Wójs A 1998 *Quantum dots* (Springer)
- [3] Sikorski C and Merkt U 1989 *Phys. Rev. Lett.* **62** 2164
- [4] Meurer B, Heitmann D and Ploog K 1992 *Phys. Rev. Lett.* **68** 1371
- [5] Maksym P A and Chakraborty T 1990 *Phys. Rev. Lett.* **65** 108
- [6] Demel T, Heitmann D, Grambow P and Ploog K 1990 *Phys. Rev. Lett.* **64** 788
- [7] Hochgräfe M, Heyn C and Heitmann D 2001 *Phys. Rev. B* **63** 035303
- [8] Krahne R, Gudmundsson V, Heyn C and Heitmann D 2001 *Phys. Rev. B*
- [9] Marlo M, Harju A and Nieminen R M 2003 *Phys. Rev. Lett.* **91** 187401
- [10] Marlo-Helle M, Harju A and Nieminen R M 2005 *Physica E* **26** 286
- [11] Chakraborty T, Halonen V and Pietiläinen P 1991 *Phys. Rev. B* **43** 14289
- [12] Pfannkuche D and Gerhardts R R 1991 *Phys. Rev. B* **44** 13132
- [13] Madhav A V and Chakraborty T 1994 *Phys. Rev. B* **49** 8163
- [14] Magnúsdóttir I and Gudmundsson V 1999 *Phys. Rev. B* **60** 16591
- [15] Ullrich C A and Vignale G 2000 *Phys. Rev. B* **61** 2729
- [16] Gudmundsson V, Manolescu A, Krahne R and Heitmann D 2002 in T Chakraborty, F Peeters and U Sivan, eds, *Nano-Physics and Bio-Electronics: A New Odyssey* (Elsevier, New York)
- [17] Chakraborty T and Pietiläinen P 2005 *Phys. Rev. Lett.* **95** 136603
- [18] García J Z, Pietiläinen P and Hyvönen P 2002 *Phys. Rev. B* **66** 195324
- [19] Harju A, Siljamäki S and Nieminen R M 2002 *Phys. Rev. Lett.* **88** 226804
- [20] Helle M, Harju A and Nieminen R M 2005 *to appear in Phys. Rev. B* **72**, cond-mat/0505314
- [21] Saarikoski H and Harju A 2005 *Phys. Rev. Lett.* **94** 246803